

submitted to J. Phys. Soc. Jpn. on 7 Feb 2001

Two-Dimensional σ -Hole Systems in Boron Layers: A First-Principles Study on $\text{Mg}_{1-x}\text{Na}_x\text{B}_2$ and $\text{Mg}_{1-x}\text{Al}_x\text{B}_2$

Shugo SUZUKI, Shin'ichi HIGAI¹, and Kenji NAKAO*Institute of Materials Science, University of Tsukuba, Tsukuba 305-8573*¹ *National Research Institute for Metals, 1-2-1 Sengen, Tsukuba 305-0047*

(Received March 7, 2019)

We study two-dimensional σ -hole systems in boron layers by calculating the electronic structures of $\text{Mg}_{1-x}\text{Na}_x\text{B}_2$ and $\text{Mg}_{1-x}\text{Al}_x\text{B}_2$. In $\text{Mg}_{1-x}\text{Na}_x\text{B}_2$, it is found that the concentration of σ holes is approximately described by $(0.8 + 0.8x) \times 10^{22} \text{ cm}^{-3}$ and the largest attainable concentration is about $1.6 \times 10^{22} \text{ cm}^{-3}$ in NaB_2 . In $\text{Mg}_{1-x}\text{Al}_x\text{B}_2$, on the other hand, it is found that the concentration of σ holes is approximately described by $(0.8 - 1.4x) \times 10^{22} \text{ cm}^{-3}$ and σ holes are disappeared at x of about 0.6. These relations can be used for experimental studies on the σ -hole systems in these materials.

KEYWORDS: MgB_2 , NaB_2 , AlB_2 , σ holes, two dimension, hole concentration

Quite recently, Nagamatsu et al. have discovered that magnesium diboride, MgB_2 , is a superconductor with a high transition temperature, T_c , of 39 K.¹⁾ Extensive studies have now started both experimentally and theoretically. In particular, since MgB_2 can be regarded as a starting material of undiscovered high T_c superconductors, it is important to search a variety of materials derived from MgB_2 .

The structure of MgB_2 consists of the layers of triangular lattices of Mg atoms and the layers of honeycomb lattices of B atoms.²⁾ This is basically the same as that of the alkali-metal binary graphite intercalation compounds (GIC).³⁾ Since Mg and B are light elements, where the s and p atomic orbitals play dominant roles, the electronic structure of MgB_2 ⁴⁾ is also very similar to those of GIC.⁵⁾ In spite of these similarity, there are no GIC superconductors with such a high T_c ; the highest T_c of alkali-metal binary GIC is only about 0.15 K for C_8K .⁶⁾

One of the outstanding differences between MgB_2 and GIC is the existence of the σ holes at the center of the Brillouin zone,⁴⁾ which are derived from the $2p_x$ and $2p_y$ atomic orbitals of B. Since the σ bands in graphite layers are energetically very deep, the generation of σ holes is extremely difficult in GIC. Furthermore, it is interesting to note that holes in boron layers will show characteristics of two-dimensional (2D) systems. As revealed so far, 2D systems can provide a rich variety of physics and

possibilities of applications. It is thus important for understanding the properties of MgB_2 and its derivatives to study the electronic structures of the σ -hole systems in boron layers.

In this Letter, we study the 2D σ -hole systems in $\text{Mg}_{1-x}\text{Na}_x\text{B}_2$ and $\text{Mg}_{1-x}\text{Al}_x\text{B}_2$ at $x=0, 1/3, 2/3$, and 1 by calculating the electronic structures of these materials based on the density functional theory. The main result of the present study is as follows. In $\text{Mg}_{1-x}\text{Na}_x\text{B}_2$, since Na is a monovalent metal, the concentration of the σ holes is increased with increasing x , approximately described by $(0.8 + 0.8x) \times 10^{22} \text{ cm}^{-3}$. In $\text{Mg}_{1-x}\text{Al}_x\text{B}_2$, on the contrary, since Al is a trivalent metal, the concentration of σ holes is decreased with increasing x , approximately described by $(0.8 - 1.4x) \times 10^{22} \text{ cm}^{-3}$. In the latter case, the σ holes are disappeared at x of about 0.6. These results can be used for experimental studies on the σ -hole systems in these materials.

In the present study, we carry out first-principles calculations based on the density functional theory with the local density approximation,⁷⁻¹⁰⁾ considering all electrons. To check the reliability of the results, the Kohn-Sham equations are solved by using both the mixed-basis method and the linear-combination-of-atomic-orbitals (LCAO) method.¹¹⁾ In this paper, we show the results obtained by the mixed-basis method although the same results can also be obtained by the LCAO method. The

cut-off energy used for plane waves is 50 eV and the atomic orbitals employed as localized orbitals are given in Table I. We use not only the atomic orbitals of neutral atoms but also those of charged atoms to increase the variational flexibility. The number of used k points in the full Brillouin zone is 52 for the structure optimization of NaB_2 and 185 for the electronic structure calculations of NaB_2 , MgB_2 , and AlB_2 . Also, that used in the calculations of $\text{Mg}_{1-x}\text{Na}_x\text{B}_2$ and $\text{Mg}_{1-x}\text{Al}_x\text{B}_2$ is 104.

Table I. Atomic orbitals used for the mixed-basis calculations.

Atom	Atomic orbitals (atomic charge)
B	$1s, 2s, 2p$ (neutral)
Na	$1s, 2s, 2p, 3s$ (neutral)
Mg	$1s, 2s, 2p, 3s$ (neutral); $3p(1+)$; $3d(2+)$
Al	$1s, 2s, 2p, 3s, 3p$ (neutral); $3d(2+)$

We first calculate the electronic structures of NaB_2 , MgB_2 , and AlB_2 . The calculations are performed at the experimental lattice constants for MgB_2 and AlB_2 ; $a = 3.084$ Å and $c = 3.522$ Å are used for MgB_2 and $a = 3.009$ Å and $c = 3.262$ Å are used for AlB_2 . On the other hand, since NaB_2 is a hypothetical material at present, it is necessary to optimize the lattice constants of this material. The resultant a and c are 3.02 Å and 4.19 Å, respectively, and are used for NaB_2 . To check the reliability of this result, we also optimized the structure of MgB_2 and found that the errors for a and c are -2% and $+0.5\%$, respectively. We thus believe that the result for NaB_2 is also reliable with the same accuracy. The lattice constants c of these materials can be understood by considering the fact that the ionic radii of Na^+ , Mg^{2+} , and Al^{3+} are 0.97 Å, 0.65 Å, and 0.50 Å, respectively.

In Figs. 1(a), 1(b), and 1(c), the calculated electronic structures of NaB_2 , MgB_2 , and AlB_2 are shown, respectively. The dotted lines in the figures are the Fermi level. The most impressive point is the position of the top of the σ bands derived from the $2p_x$ and $2p_y$ atomic orbitals of B. In NaB_2 and MgB_2 , the top of the σ bands are above the Fermi level and accordingly there exist σ holes in these materials. This is in strong contrast to the fact that there are no σ holes in GIC. Since Na is a monovalent metal while Mg is a divalent metal, the concentration of σ holes is larger in NaB_2 than in MgB_2 . Thus the concentration of the σ holes can be increased when we increase x in $\text{Mg}_{1-x}\text{Na}_x\text{B}_2$. On the contrary, in AlB_2 , the top of the σ bands is below the Fermi level

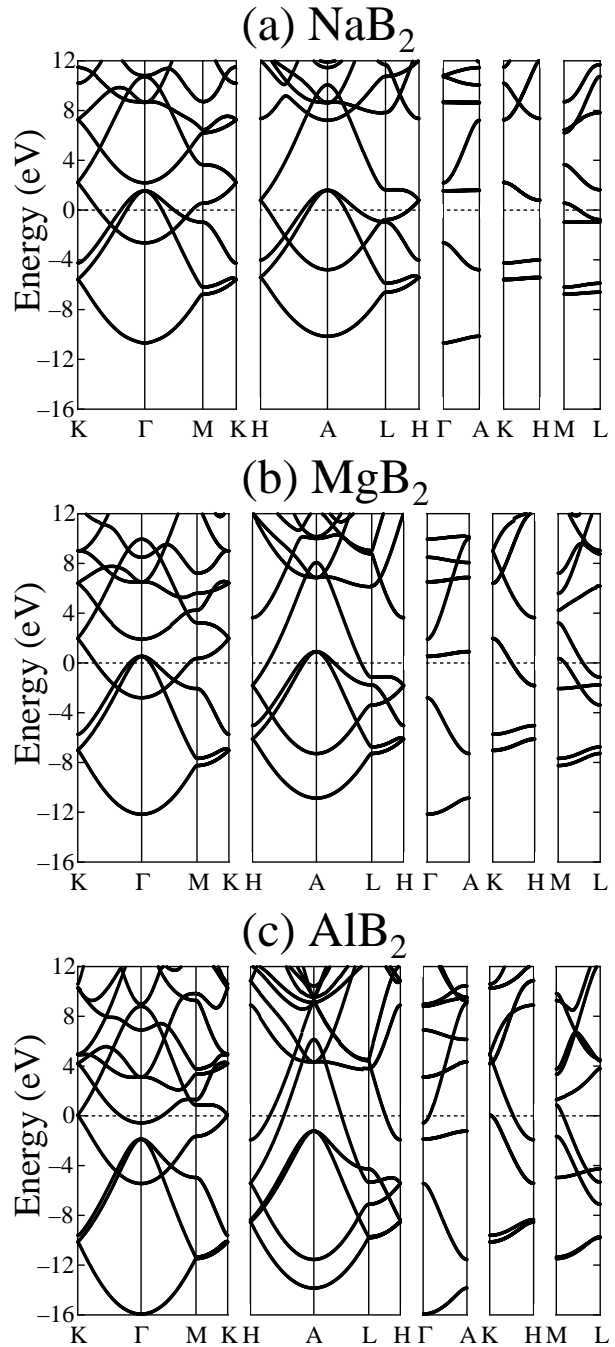


Fig. 1. Band structures of (a) NaB_2 , (b) MgB_2 , and (c) AlB_2 . The dotted lines show the Fermi level.

and accordingly there are no σ holes in this material. Thus the σ holes are decreased when we increase x in $\text{Mg}_{1-x}\text{Al}_x\text{B}_2$ and eventually they are disappeared at a certain value of x .

Furthermore, since the dispersion of the top of the σ bands of all the materials is very small along the Γ -A direction, the σ holes can show characteristics of 2D systems such as large fluctuation, etc. This is in strong contrast to the three dimensionality of the other carriers in these materials. In all the materials, there exist three-dimensional (3D) π electrons and/or holes. Also, in AlB_2 , there exist small number of 3D electrons in the nearly free electron state at the Γ point, which is derived from the hybridization between the $3s$ atomic orbitals of Al and the interlayer state of boron layers; this is very similar to the situation in C_8K , where the nearly free electrons also exist at the Γ point.¹²⁾ It should be noted that, in GIC, there exist π electrons and/or holes and also nearly free electrons and not the σ holes.

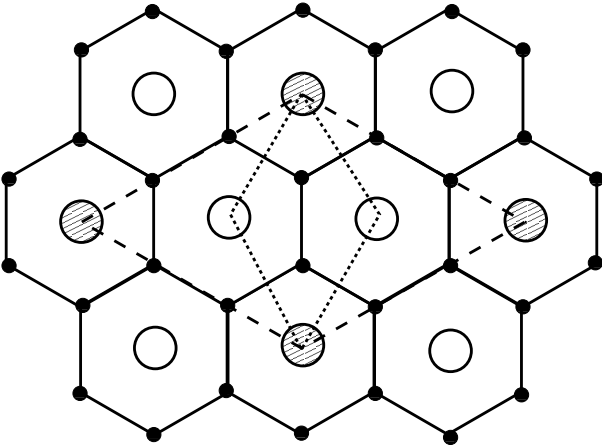


Fig. 2. In-plane ($\sqrt{3} \times \sqrt{3}$) structure (dashed lines) used in the electronic structure calculations of $\text{Mg}_{1-x}\text{M}_x\text{B}_2$ ($M=\text{Na}$ or Al , $x=0, 1/3, 2/3$, and 1) and original (1×1) structure (dotted lines). Small closed circles represent B atoms and large circles represent the other atoms. For $x=0$, all the large circles are Mg atoms. For $x=1/3$, open and hatched circles are Mg and M atoms, respectively. For $x=2/3$, open and hatched circles are M and Mg, respectively. For $x=1$, all the large circles are M atoms.

Next, we study the electronic structures of $\text{Mg}_{1-x}\text{Na}_x\text{B}_2$ and $\text{Mg}_{1-x}\text{Al}_x\text{B}_2$ at $x=0, 1/3, 2/3$, and 1 . In the calculations, we assume the in-plane ($\sqrt{3} \times \sqrt{3}$) structure as shown in Fig. 2. This structure has a simplicity that the threefold rotation axis also exists as in the (1×1) original

structure and thus the same Brillouin zone can be used. We also assumed that the lattice constants of these materials can be obtained by linearly interpolating between the lattice constants of MgB_2 and NaB_2 or AlB_2 . As an example, we show the result for $\text{Mg}_{2/3}\text{Na}_{1/3}\text{B}_2$ in Fig. 3. The obtained electronic structure can be understood by considering the folding of the original band structures shown in Fig. 1. The σ bands are easily identified by observing that they are the bands with small dispersion along the Γ -A direction just above the Fermi level.

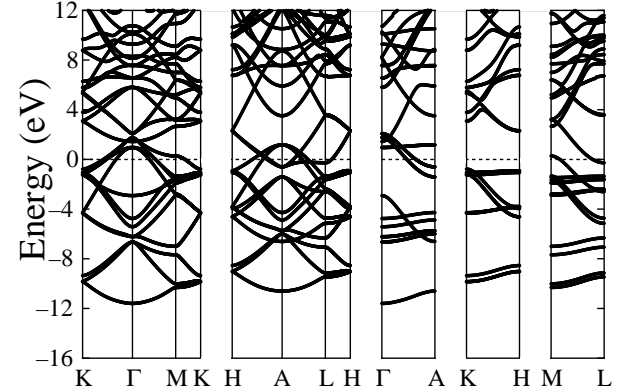


Fig. 3. Band structure of $\text{Mg}_{2/3}\text{Na}_{1/3}\text{B}_2$. The dotted line shows the Fermi level.

In Fig. 4, we show the top of the σ bands in $\text{Mg}_{1-x}\text{Na}_x\text{B}_2$ and $\text{Mg}_{1-x}\text{Al}_x\text{B}_2$ as a function of x . The dotted line in the figure shows the Fermi level. It is found that the dependence is monotonous and the largest attainable value is 1.8 eV for NaB_2 . We also find that, in $\text{Mg}_{1-x}\text{Al}_x\text{B}_2$, the top of the σ bands is below the Fermi level for x larger than about 0.6 , that is, the σ holes are disappeared for such x . The dependence on x for the entire region from NaB_2 to AlB_2 via MgB_2 shown in Fig. 4 cannot be fit with a single straight line. It is necessary to fit the result with a curve or, at least, with two straight lines, one for $\text{Mg}_{1-x}\text{Na}_x\text{B}_2$ and the other for $\text{Mg}_{1-x}\text{Al}_x\text{B}_2$. If we select the latter choice, the result can be fit with

$$\varepsilon_{\text{top}} = 0.90 + 0.91x \text{ eV} \quad (1)$$

for $\text{Mg}_{1-x}\text{Na}_x\text{B}_2$ and with

$$\varepsilon_{\text{top}} = 0.90 - 1.57x \text{ eV} \quad (2)$$

for $\text{Mg}_{1-x}\text{Al}_x\text{B}_2$. Here, we ignore the point for AlB_2 in

obtaining the above formula because some quantities, including the top of the σ bands and the cohesive energy as shown below, are not on the same straight line as the other $\text{Mg}_{1-x}\text{Al}_x\text{B}_2$ are; this can be ascribed to the existence of the nearly free electrons in AlB_2 which do not exist in the other $\text{Mg}_{1-x}\text{Al}_x\text{B}_2$ calculated in the present study.

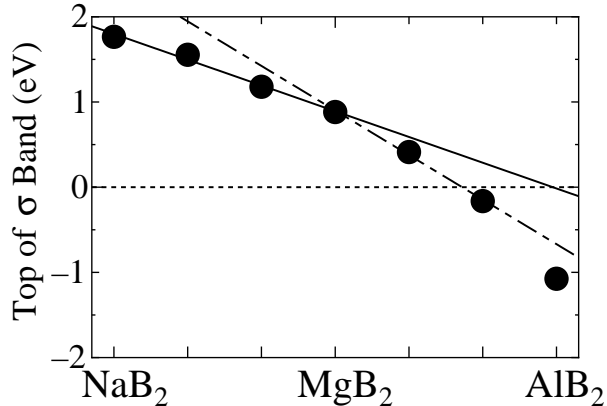


Fig. 4. Top of the σ bands as a function of x . The horizontal axis is from NaB_2 to AlB_2 via MgB_2 . The dotted line shows the Fermi level. The solid line fits the four points for $\text{Mg}_{1-x}\text{Na}_x\text{B}_2$. The dotted-dashed line fits the three points for $\text{Mg}_{1-x}\text{Al}_x\text{B}_2$, ignoring the point for AlB_2 .

In Fig. 5, we show the cohesive energy of $\text{Mg}_{1-x}\text{Na}_x\text{B}_2$ and $\text{Mg}_{1-x}\text{Al}_x\text{B}_2$ as a function of x . It is found that the most stable material is AlB_2 and the least stable one is NaB_2 . The dependence on x for the entire region from NaB_2 to AlB_2 via MgB_2 can be described by a single straight line if we ignore the point for AlB_2 because the cohesive energy may be affected by the existence of the nearly free electrons as mentioned above. The result can be fit with

$$E_c = 5.59 - 0.62x \text{ eV/atom} \quad (3)$$

for $\text{Mg}_{1-x}\text{Na}_x\text{B}_2$ and with

$$E_c = 5.59 + 0.62x \text{ eV/atom} \quad (4)$$

for $\text{Mg}_{1-x}\text{Al}_x\text{B}_2$. Although NaB_2 is a hypothetical material at present, we believe that this material can be synthesized in some appropriate conditions because the cohesive energy of NaB_2 , about 5 eV/atom, is not so small; it is almost the same as that of the bulk Si.

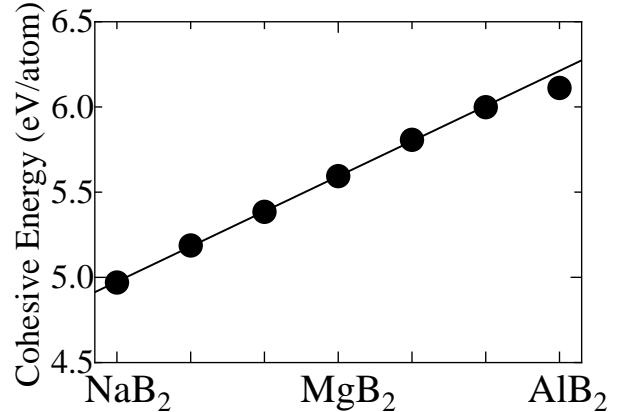


Fig. 5. Cohesive energy as a function of x . The horizontal axis is from NaB_2 to AlB_2 via MgB_2 . The solid line fits the six points for $\text{Mg}_{1-x}\text{Na}_x\text{B}_2$ and $\text{Mg}_{1-x}\text{Al}_x\text{B}_2$, ignoring the point for AlB_2 .

Next we study the dependence of the concentration of σ holes on x , assuming constant density of states for the upper region of the σ bands. This assumption is good as far as two conditions are satisfied; one is that the dispersion along the Γ -A direction is very small and the other is that the deviation from the in-plane free-electron-like dispersion is negligible. Since both conditions are satisfied as shown in Fig. 1, we derive the formula which give the concentration of σ holes for given x . First, it is necessary to fit the in-plane free-electron-like dispersion by using effective masses for heavy and light holes. As a result, we find that the effective mass for heavy holes is $0.5m_e$ and that for light holes is $0.3m_e$, where m_e is the mass of free electrons. Next, combining with the results shown in Fig. 4, the following formula are derived for the concentration of the σ holes:

$$n_h = (0.8 + 0.8x) \times 10^{22} \text{ cm}^{-3} \quad (5)$$

for $\text{Mg}_{1-x}\text{Na}_x\text{B}_2$ and

$$n_h = (0.8 - 1.4x) \times 10^{22} \text{ cm}^{-3} \quad (6)$$

for $\text{Mg}_{1-x}\text{Al}_x\text{B}_2$. Thus, in $\text{Mg}_{1-x}\text{Na}_x\text{B}_2$, the largest attainable concentration of σ holes is about $1.6 \times 10^{22} \text{ cm}^{-3}$ in NaB_2 . In $\text{Mg}_{1-x}\text{Al}_x\text{B}_2$, on the other hand, σ holes are disappeared at x of about 0.6.

Here, we discuss the possibility of LiB_2 as a candidate to increase the concentration of σ holes. Although one may expect that LiB_2 is the most plausible candidate because of almost the same ionic radius of Li^+ , 0.68 \AA , as that of Mg^{2+} , this may not the case. We have found

that the structure optimization of LiB_2 results in strong contraction of c , which is found to be less than 3 Å. The result strongly conflicts to a simple expectation that the lattice constant c of LiB_2 should be about 3.6 Å if we estimate it by considering the ionic radius of Li^+ . To elucidate stable structure of LiB_2 , our study is now in progress. In spite of this result, one can still expect that $\text{Mg}_{1-x}\text{Li}_x\text{B}_2$ for sufficiently small x can be synthesized because the introduction of sufficiently small Li cannot affect the lattice constant c so strongly.

We next discuss the difference between MgB_2 and other metal diborides such as transition-metal (TM) diborides¹³⁾ and noble-metal diborides, AgB_2 and AuB_2 . The most important point is the absence of d atomic orbitals in MgB_2 in contrast to the existence of d atomic orbitals in other metal diborides. In particular, since the d atomic orbitals in TM are partly filled, they form strong covalent bonding with σ bonds of boron layers. This can destroy 2D σ -hole system in boron layers; we have calculated the electronic structures of some TM diborides and have found that the σ bands of boron layers are strongly affected by the covalent bonding with d atomic orbitals of TM. On the other hand, AgB_2 and AuB_2 can be candidates for similar materials as MgB_2 . The reason for this is that the σ holes may survive in these materials because d atomic orbitals in these materials should be sufficiently lower than the Fermi level and thus the hybridization between the d atomic orbitals and the σ bands may occur at a lower-energy region.

We finally discuss a possible relation between the superconductivity in MgB_2 and the 2D σ -hole systems in boron layers. If the superconductivity is disappeared in $\text{Mg}_{1-x}\text{Al}_x\text{B}_2$ at x of about 0.6, it should be caused by the σ -hole systems. In addition, there are no TM diborides with T_c as high as that of MgB_2 ; this may be understood because they have no σ holes. If this is the case, both of the electron-phonon interaction and the electron correlation can be the likely origin of the superconductivity. Since σ bonds, especially those of B, C, N, and O, are very strong, the interaction between the σ holes and the in-plane σ -bond vibration is expected to be very strong, too. Furthermore, this electron-phonon coupling can result in a superconductivity of high T_c because the frequency of the σ -bond vibration is of the order of 0.2 eV. On the other hand, the electron correlation in the σ holes seems also important for the properties of the σ -hole system in MgB_2 because the wave function of the σ holes is localized to considerable degree.

Acknowledgements

We would like to thank J. Akimitsu, T. Arima, and H. Tsunetsugu for useful discussions.

-
- 1) J. Nagamatsu, N. Nakagawa, T. Muranaka, Y. Zenitani, and J. Akimitsu: submitted to Nature.
 - 2) V. Russell, R. Hirst, F. A. Kanda and A. J. King: *Acta. Cryst.* **6** (1953) 870.
 - 3) M. S. Dresselhaus and G. Dresselhaus: *Adv. Phys.* **30** (1981) 139.
 - 4) D. R. Armstrong and P. G. Perkins: *J. Chem. Soc., Faraday Trans. 2* **75** (1979) 12.
 - 5) N. A. W. Holzwarth: *Graphite Intercalation Compounds II*, ed. H. Zabel and S. A. Solin (Springer Verlag, Berlin, 1992) p. 7.
 - 6) S. Tanuma: *Graphite Intercalation Compounds II*, ed. H. Zabel and S. A. Solin (Springer Verlag, Berlin, 1992) p. 163.
 - 7) P. Hohenberg and W. Kohn: *Phys. Rev.* **136** (1964) B864.
 - 8) W. Kohn and L. J. Sham: *Phys. Rev.* **140** (1965) A1133.
 - 9) J. P. Perdew and A. Zunger: *Phys. Rev. B* **23** (1981) 5048.
 - 10) D. M. Ceperley and B. J. Alder: *Phys. Rev. Lett.* **45** (1980) 566.
 - 11) S. Suzuki and K. Nakao, *J. Phys. Soc. Jpn.* **69** (2000) 532.
 - 12) S. Amamiya, S. Higai, S. Suzuki, and K. Nakao: *Mol. Cryst. Liq. Cryst.* **340** (2000) 53.
 - 13) P. Vajeeston, P. Ravindran, C. Ravi and R. Asokamani: *Phys. Rev. B* **63** (2001) 45115.